Local and Global Response Simulation of a Reinforced Concrete Wall Specimen

F. Dashti
University of Wollongong, Australia

S. Malekpour
University of Tabriz, Iran

A. Davaran
Ecole Polytechnique, Montreal, Canada

SUMMARY:
In this study, efficiency of a simple macroscopic model in predicting the nonlinear response of a reinforced concrete shear wall specimen tested under monotonic loading is evaluated. The model consists of nonlinear spring elements representing flexural and shear behavior. The model was implemented in ABAQUS6.6, and the analysis results show excellent agreement with experimental measurements of the specimen. The experimental and analytical responses were compared both globally and locally. The global parameters include lateral load – top displacement, lateral load – top flexural displacement, lateral load – top shear displacement and drift profiles of the specimen. The local parameters consist of neutral axis position at different stages of loading and lateral load versus axial displacement response of the first story boundary elements.
Nonlinear response of the elements constituting the wall boundary elements representing behavior of reinforcing steel and confined concrete is compared with the experimental observations such as concrete cracking and reinforcement yielding.

Keywords: Shear Wall, Macroscopic model, Test specimen, Local behavior, Global behavior.

1. INTRODUCTION

The proposed procedures for analytical modeling of an RC shear wall can be classified into two broad groups, microscopic and macroscopic models. Considering all the aspects of both procedures, especially practicality and efficiency, using macro models to predict the lateral load-displacement response of shear wall buildings has always been preferable to spending much time on developing microscopic models.
Orakcal et al. [1] used a multiple spring macro-model and adopted hysteretic constitutive laws of concrete and steel for the springs. The tension stiffening effects were directly incorporated into the constitutive stress-strain relations implemented for concrete and steel. The model was calibrated, and validated against extensive experimental data at both local and global response levels by Orakcal and Wallace [2]. Jalali and Dashti [3], [4] evaluated efficiency of the macroscopic model investigated by Orakcal and Wallace [2] in predicting the nonlinear behavior of two slender RC walls subjected to monotonic loading, and investigated its advantages and deficiencies in comparison with the microscopic models following a 2D analysis of the selected test specimens using the finite element approach, and assessed the sensitivity of both procedures to modeling parameters. In this study the capability of the macroscopic model in predicting the local and global response of one of the test specimens investigated in previous studies is comprehensively investigated.

2. GENERAL DESCRIPTION OF THE MACRO MODEL

The macro model adopted here is composed of several macro elements, the number of which depends on the expected accuracy and local behavior. Each macro element (Fig. 2.1.) consists of vertical spring elements connected to rigid beams at the top and bottom levels, representing the flexural response and a horizontal spring element, placed at the height ch, simulating the shear behavior of an RC wall. As

shown in Fig. 2.1., two parallel spring elements representing the uniaxial behavior of concrete and steel are used to define the uniaxial behavior of the tributary area assigned to each couple of springs. The strains in concrete and steel are typically assumed to be equal (perfect bond) within each uniaxial element. Detailed description of the model and the constitutive models of materials is given by Jalali and Dashti [3], [4]. The only parameters associated with the analytical wall model are the number of uniaxial elements used along the length of the wall cross section (n), the number of MVLEM elements stacked on top of each other along the height of the wall (m), and the parameter defining the location of the center of rotation along the height of each MVLEM element (c) (Orakcal et al. [5]). The value of c = 0.4 recommended by Vulcano et al. [6] based on comparison of the model response with experimental results has been used to define the location of the center of rotation along the height of each macro element.

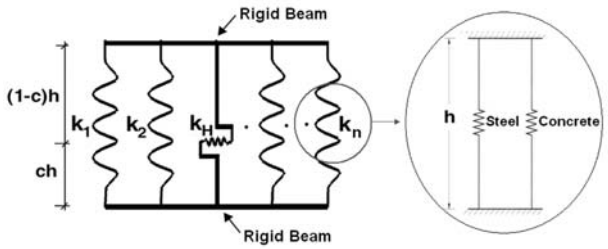

Figure 2.1. A macro element

3. TEST SPECIMEN

The three-story wall specimen tested by Vallenas et al. [7] has been used to calibrate and assess the analytical model. The specimen selected is a framed wall where the boundary elements protrude from the surface of the wall (SW3) (Fig. 3.1.). The wall was intended to idealize the three lower stories of a framed wall designed for a ten-story building. The specimen was subjected to monotonic loading (Fig. 2).

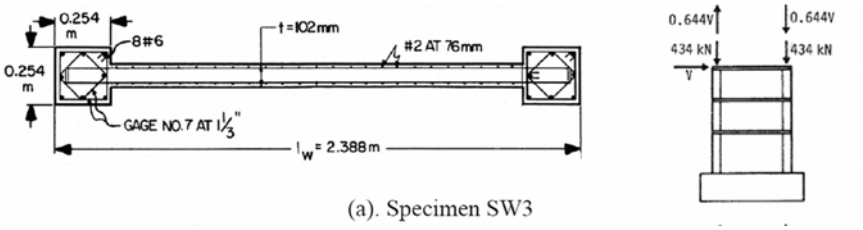

Figure 3.1. Geometrical properties and loading patterns of the specimen

4. ANALYTICAL VERSUS EXPERIMENTAL RESPONSES OF THE SPECIMEN

The computed lateral force-deformation diagram for Specimen SW3 is shown in Fig. 4.1. There are changes in the slope of the diagram at points A, B, C, D, E, F and G which are corresponding to changes in the behavior of the spring elements representing the axial behavior of the boundary elements and shear behavior of the first story. The lateral load versus axial displacement response of the first story boundary elements is shown in Fig. 4.2. Using the axial displacements corresponding to the points mentioned before and the axial load-displacement response of the spring elements constituting the first story boundary elements indicated in Figs. 4.3 and 4.4, the changes in the behavior of the concrete and reinforcement of the first story boundary elements at these points can be determined (the points corresponding to significant changes in the slope of the diagrams are magnified in Figs. 4.3., 4.4. and 4.5.). The load-displacement response of the shear spring element of the first

story is displayed in Fig. 4.5. Deformation pattern of the macroscopic model of Specimen SW3 at different stages of loading can be observed in Fig. 4.6.

At Point A the axial displacement of the first story tension column is 0.18mm (Fig. 4.2.(a)), at which as shown in Fig. 3(a) the spring element corresponding to the concrete of the first story tension column reaches its cracking strength. Deformation pattern of Specimen SW3 at Point A (Fig. 4.6.(a)) shows no change in the neutral axis position. The second change in the overall force-deformation diagram can be observed at Point B, which is accompanied by an initial change in the slope of the axial force-deformation diagram representing the axial response of the reinforcement of the first story tension column, which yields completely at Point C (Fig. 4.3.(b)), and leads to a small change in the neutral axis position (Fig. 4.6.(b)). The same process can be observed in the behavior of the reinforcement of the first story compression column at Points D and E, (Fig. 4.4.(b)). At Point D (Fig. 4.1.), overall yielding of the model takes place. The deformation pattern of the model at Point E (Fig. 4.6.(c)) indicates the relatively great change in the neutral axis position. At Point F the spring element representing the axial behavior of the confined concrete of the first story compression column reaches its compressive strength (Fig. 4.4.(a)), and finally at Point G, as shown in Fig. 4.5., the shear yielding in the horizontal spring element representing the shear behavior of the first story can be observed. Deformation pattern of Specimen SW3 before and after shear yielding is shown in Figs. 4.6.(d) and 4.6.(e).

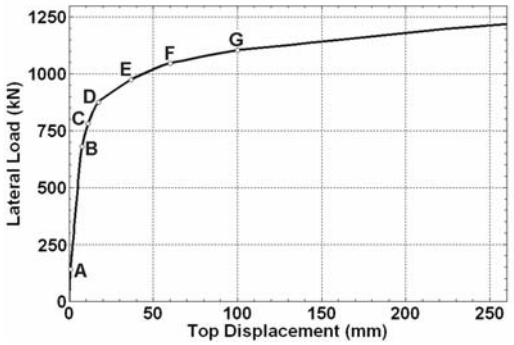

Figure 4.1. Lateral load versus top displacement response of the specimen.

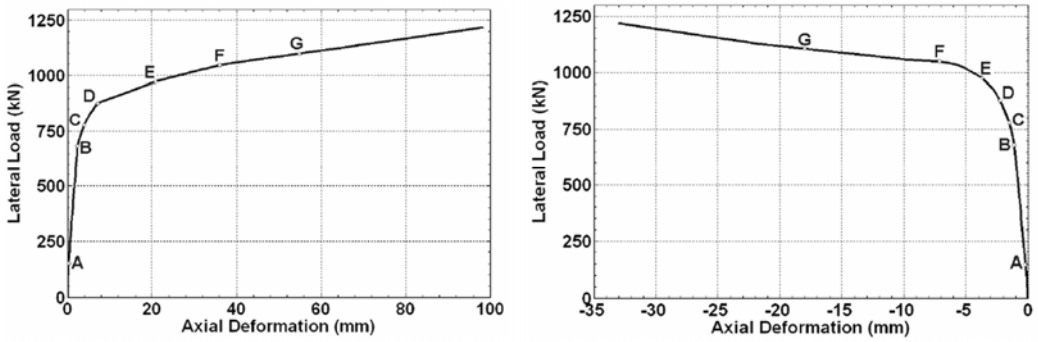

(a) Tension column (b) Compression column

Figure 4.2. Lateral load versus axial displacement response of the 1st boundary elements.

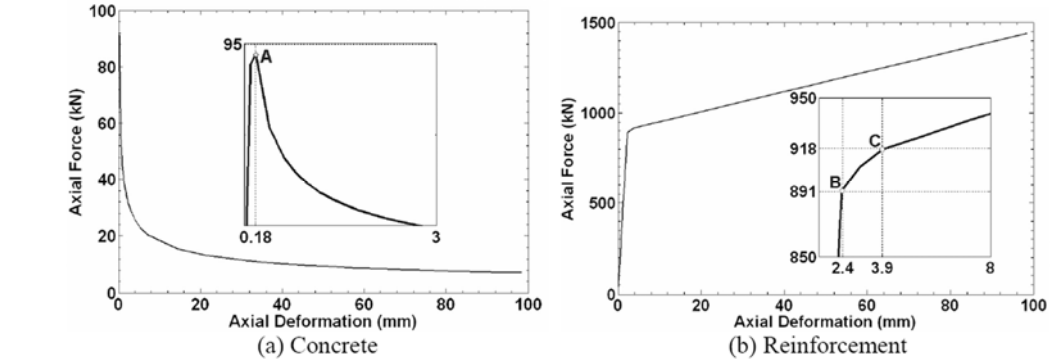

Figure 4.3. Axial load-displacement response of the spring elements of the 1st story tensile column

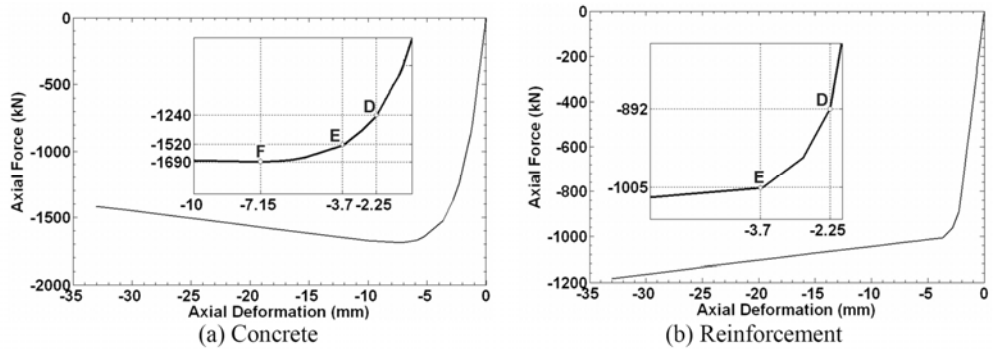

Figure 4.4. Axial load-displacement response of the spring elements of the 1st story compressive column

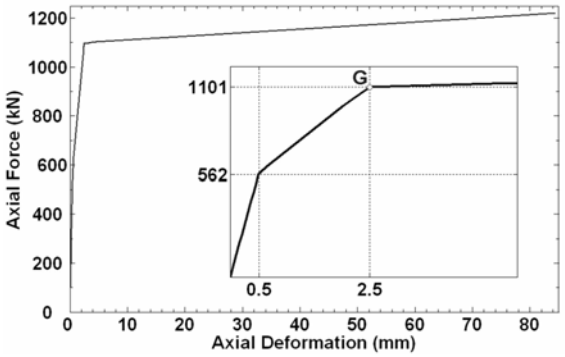

Figure 4.5. Axial load-displacement response of the 1st story shear spring element

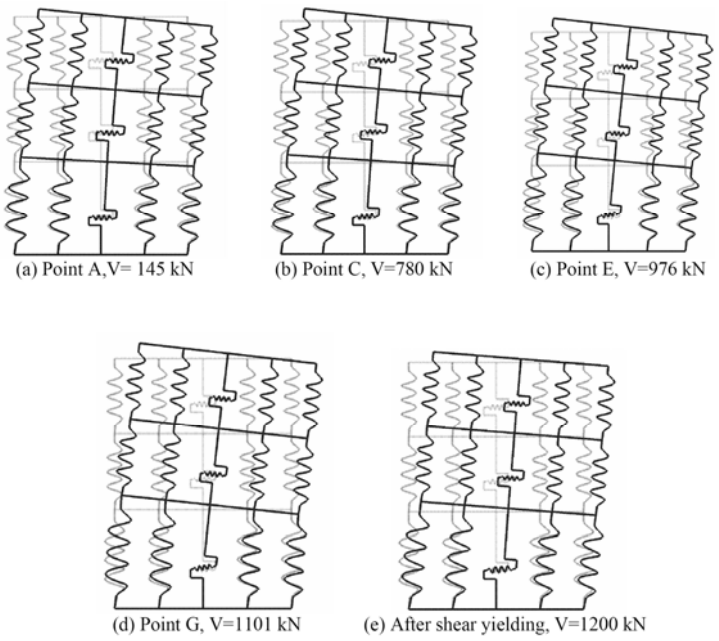

Figure 4.6. Deformation pattern of the macroscopic model of Specimen SW3 at different stages of loading

Migration of the neutral axis along the wall cross section during loading is indicated for analytical and experimental models in Figs. 9 and 10. The neutral axis position at different stages of loading of the macro model is indicated via ellipses in Fig. 9, and is in good agreement with the experimental measurement of the neutral axis position, shown in Fig. 10.

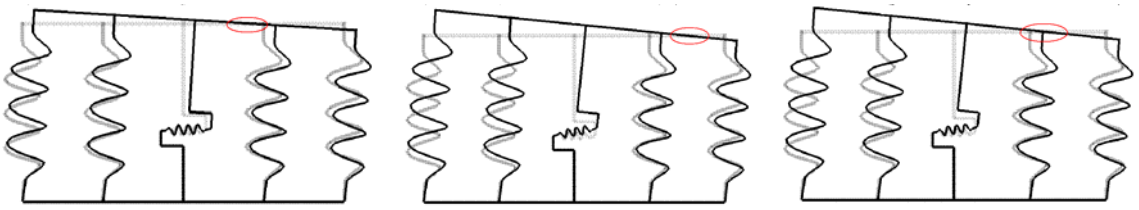

Figure 4.7. Migration of the neutral axis along the wall cross section during loading (Analytical model)

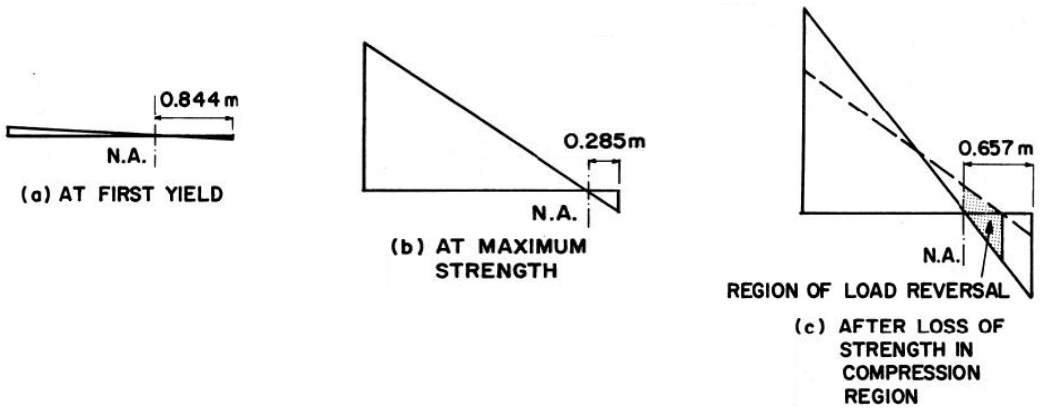

Figure 4.8. Migration of the neutral axis along the wall cross section during loading (Experimental model) [7]

Figs. 4.9., 4.10. and 4.11. compare the measured and predicted lateral load – top displacement, lateral load – top flexural displacement and lateral load – top shear displacement responses of the specimen. The analytical model provides a good prediction of the wall lateral overall and flexural displacement, and the discrepancy observed between analytical and experimental lateral load-top shear displacement can be attributed to considering uncoupled shear and flexural responses in the analytical model. In other words, using the origin-oriented-hysteresis model to define the behavior of the horizontal spring elements, the interaction between shear and flexural response components observed even in relatively slender RC walls has not been considered in the analytical model.
According to the experimental results (Vallenas et al. [7]), at point 49 (Fig. 4.9.(a)) overall yielding Specimen SW3 takes place. This is the point at which all the reinforcement in the column cross-section at the base of the tension column yields. The nominal displacement ductility ratio of one, obtained from the overall force deformation diagram (Fig. 4.9.(a)), was taken 18 mm at a lateral load of 898 kN (Point 49). At a nominal displacement ductility level of three (lateral displacement at the third floor $\delta_3 = 54\,mm$), and a lateral load of 996 kN, spalling initiated at the base of the compression column (Point 52, Fig. 4.9.(a)). After an interruption in the test, the specimen reached a peak load of 1090 kN (Point 75). Soon afterwards, the cover at the base of the compression column completed spalling with the longitudinal reinforcement buckling, and confining hoops at the base of the compression column rupturing. The analytical model predicts yielding of the first story tensile reinforcement at Point C (V= 780 kN), yielding initiation of the first story compressive reinforcement at Point D (V=878 kN), maximum compressive strength of the first story compression column concrete at Point F (V=1048 kN) and shear yielding of the first story at Point G (V=1101 kN).

Comparing the experimental and predicted behavior of the specimen, it can be concluded that the analytical model is sufficiently accurate in predicting the global response of an RC wall, is able to simulate the response of different elements of an RC wall to monotonic loading and can be used to determine the effect of the axial behavior of the elements constituting an RC wall on its global response, by which the optimum amount and properties for reinforcement and concrete of different sections can be defined.

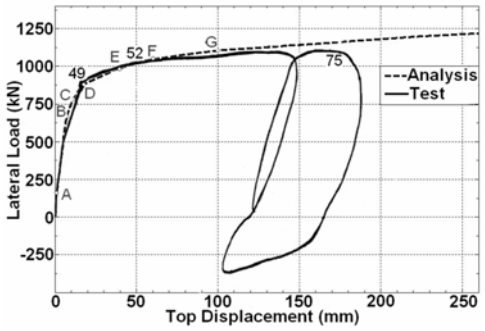

Figure 4.9. Lateral load – top displacement response of the specimen

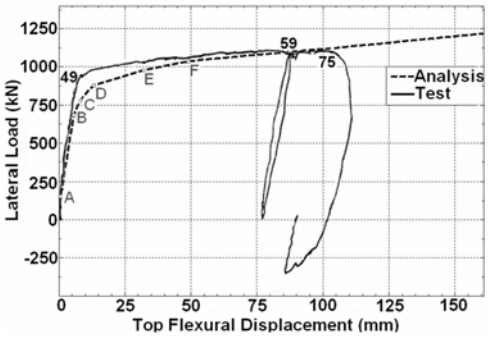

Figure 4.10. Lateral load – top flexural displacement response of specimens

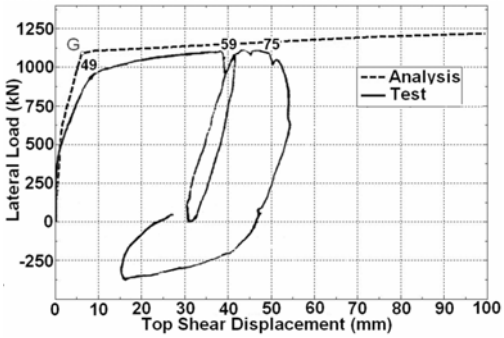

Figure 4.11. Lateral load – top shear displacement response of specimens

Table 4.1. indicates the analytical inter-story and overall drift values of the specimen, and the experimental drift values at corresponding points are shown in Table 4.2. The analytical drift values are in good agreement with the experimental ones.

Table 4.1. Inter-story and overall drift of the analytical model

Points	1st Story	2nd Story	3rd Story	Overall Drift
A	0.00021	0.0003551	0.000425	0.0003194
B	0.001691	0.002841	0.003455	0.002576
C	0.002567	0.004178	0.004899	0.003765
D	0.00398	0.00641	0.007237	0.005704
E	0.008654	0.01408	0.01501	0.01223
F	0.01412	0.02316	0.02421	0.01993
G	0.02557	0.03843	0.03961	0.03374
V=1137kN	0.04881	0.04641	0.04767	0.04773
V=1169kN	0.07221	0.05418	0.0554	0.06163

Table 4.2. Inter-story and overall drift of the experimental model [7]

Specimen (Load Pt.)	Stage	1st Story	2nd Story	3rd Story	Overall Drift
3 monotonic	1st Yield	0.0039	0.0046	0.0048	0.0044
(75)	Max. Str.	0.0550	0.0569	0.0600	0.0574
(76)	Max. Displ.	0.0623	0.0589	0.0628	0.0614

5. CONCLUDING REMARKS

In this study, reliability of a simple macroscopic model for nonlinear behavior simulation of reinforced concrete shear walls is investigated much more comprehensively using local and global parameters.
The model could favorably predict the lateral load-top displacement, lateral load-top flexural displacement, lateral load-top shear displacement in addition to inter-story and overall drift ratios of the test specimen. These parameters can be deemed as global parameters as they concern the response of the whole model in contrast with local parameters that address the response of the elements constituting the model during the loading period.
The factors investigated as local parameters include nonlinear response of the spring elements forming the model and migration of the neutral axis position during loading. Nonlinear behavior of the spring

elements at 1st story is compared with the corresponding elements and regions of the test specimen at points of noticeable change in slope of the lateral load-top displacement response of the model indicating a favorable agreement between analytical and experimental observations. Also, the schematic view of the neutral axis position was in favorable agreement with the experimental measurements.

The model relates the predicted flexural response directly to uniaxial material behavior without incorporating any additional empirical relations. Furthermore, obtaining the uniaxial response of the spring elements of the model allows the designer to predict the influence of amount and physical properties of the materials on both local and global response of an RC wall.

REFERENCES

[1] Orakcal, K. Conte, JP. Wallace, JW. (2004). "Flexural Modeling of Reinforced Concrete Walls- Model Attributes", *ACI Struct J* **2004;101(5),** 688 – 698.

[2] Orakcal, K. Wallace, JW. (2006) "Flexural Modeling of Reinforced Concrete Walls-Model Calibration", *ACI Struct J* **2006;103(2)**, 196 – 206.

[3] Dashti, F. (2008) " A Practical Model for Seismic Analysis of Reinforced Concrete Shear Walls", *MSc dissertation, University of Tabriz, Iran*, 150 pp.

[4] Jalali, A. Dashti, F. (2010) "Nonlinear Behavior of Reinforced Concrete Shear Walls Using Macroscopic and Microscopic Models", *J Engng Struct* **32 (2010)**, 2959_2968.

[5] Orakcal, K. Massone, LM. Wallace, JW. (2006) "Analytical Modeling of Reinforced Concrete Walls for Predicting Flexural and Coupled Shear-Flexural Responses", Report No. *PEER* **2006/07**, PEER, University of California, Berkeley, 2006.

[6] Vulcano, A. Bertero, VV. Colotti, V. (1988) "Analytical modeling of RC structural walls", Proceedings, *9th World Conference on Earthquake Engineering* **(6)**, Tokyo-Kyoto, Japan.

[7] Vallenas, JM. Bertero, VV. Popov, EP. (1979) "Hysteretic behavior of reinforced concrete structural walls", Report No. *UCB/EERC*-**79/20**, EERC, University of California, Berkeley, California.1-268.